Protein concentration gradients and switching diffusions

Paul C. Bressloff, Sean D. Lawley, and Patrick Murphy

Phys. Rev. E **99**, 032409 — Published 7 March 2019

DOI: 10.1103/PhysRevE.99.032409

Protein concentration gradients and switching diffusions

Paul C. Bressloff, Sean D. Lawley and Patrick Murphy
Department of Mathematics, University of Utah, Salt Lake City, UT 84112 USA
(Dated: February 19, 2019)

Morphogen gradients play a vital role in developmental biology by enabling embryonic cells to infer their spatial location and determine their developmental fate accordingly. The standard mechanism for generating a morphogen gradient involves a morphogen being produced from a localized source and subsequently degrading. While this mechanism is effective over the length and time scales of tissue development, it fails over typical subcellular length scales due to the rapid dissipation of spatial asymmetries. In a recent theoretical work, we found an alternative mechanism for generating concentration gradients of diffusing molecules, in which the molecules switch between spatially constant diffusivities at switching rates that depend on the spatial location of a molecule. Independently, an experimental and computational study later found that *C. elegans* zygotes rely on this mechanism for cell polarization. In this paper, we extend our analysis of switching diffusivities to determine its role in protein concentration gradient formation. In particular, we determine how switching diffusivities modifies the standard theory, and show how space-dependent switching diffusivities can yield a gradient in the absence of a localized source. Our mathematical analysis yields explicit formulas for the intracellular concentration gradient which closely match the results of previous experiments and numerical simulations.

I. INTRODUCTION

It is well known that at the tissue level protein (morphogen) concentration gradients play a crucial role in the spatial regulation of patterning during development [1, 2]. That is, a continuously varying morphogen concentration drives a corresponding spatially discrete variation in gene expression through some form of concentration thresholding. The most common mechanism of morphogen gradient formation is thought to involve a localized source of protein production within the embryo, combined with diffusion away from the source and subsequent degradation [3, 4]. Historically speaking, the idea that a reaction-diffusion system can spontaneously generate spatiotemporal patterns was first introduced by Turing in his seminal 1952 paper [5]. Turing considered the general problem of how organisms develop their structures during the growth from embryos to adults. He established the principle that two nonlinearly interacting chemical species differing significantly in their rates of diffusion can amplify spatially periodic fluctuations in their concentrations, resulting in the formation of a stable periodic pattern. The Turing mechanism for morphogenesis was subsequently refined by Gierer and Meinhardt [6], who showed that one way to generate a Turing instability is to have an antagonistic pair of molecular species, a slowly diffusing chemical activator and a quickly diffusing chemical inhibitor, which they applied to a number of specific biological systems. Over the years, the range of models and applications of the Turing mechanism expanded dramatically [7], in spite of the fact that most experimental findings suggested that morphogenesis was guided by morphogen concentration gradients. Indeed, for many years the only direct experimental evidence for Turing-like patterning of molecular concentrations came from the inorganic Belousov-Zhabotinsky reaction [8]. This changed when Kondo and Asai demonstrated the occurrence of the Turing mechanism in studies of coat patterning in angel fish [9].

Advances in live cell imaging and gene knockout protocols are now allowing for a closer connection between theories of pattern formation and cell biology, based either on the Turing mechanism or on the formation of protein concentration gradients. Indeed, it has been found that pattern formation can also occur at the intracellular level. However, the standard mechanisms for generating robust and persistent patterns over the length scales of tissue development tend to fail over typical subcellular length scales (0.1-10 μm) [10, 11]. This has generated considerable interest in identifying subcellular mechanisms for pattern formation. One recent example concerns intracellular protein concentration gradient formation during the asymmetric division of the Caenorhabditis elegans (*C. elegans*) zygote, that is, the fertilized egg cell [12]. In the experimental study of Wu et al. [12], a pair of RNA-binding proteins MEX- 5 and PIE-1 formed opposing subcellular concentration gradients in the absence of a local source due to a spatially heterogeneous switching process. That is, both proteins switched between fast-diffusing and slow-diffusing states on timescales that were much shorter (seconds) than the timescale of gradient formation (minutes). Moreover, the switching rates were strongly polarized along the anterior/posterior axis of the zygote such that fast-diffusing MEX-5 and PIE-1 proteins were approximately symmetrically distributed, whereas the corresponding slow-diffusing proteins were highly enriched in the anterior and posterior cytoplasm, respectively.

We previously proposed a theoretical model of space-dependent switching diffusivities [13, 14], similar to the mechanism observed experimentally by Wu et al. [12]. In particular, we considered a Brownian particle that randomly switches between two distinct conformational states with different diffusivities, see Fig. 1. In each state

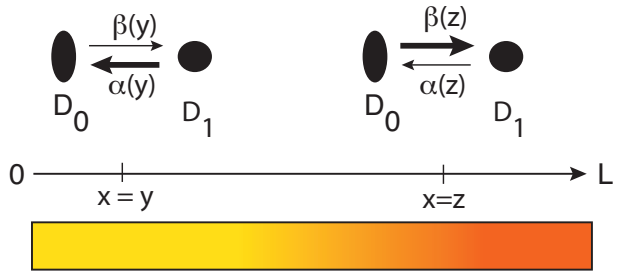

FIG. 1. Schematic illustration of heterogeneous diffusion due to temporal disorder. A Brownian particle randomly switches between two conformational states $n = 0, 1$ having different diffusivities such that $D_0 < D_1$. The switching rates $\alpha(x), \beta(x)$ are taken to be dependent on spatial position x, $0 \leq x \leq L$. In this particular example, the relative rate of switching $\beta(x)/\alpha(x)$ increases to the right as indicated by the color gradient. Hence, the particle spends more time in the slow diffusing state at the end $x = 0$ and more time in the fast diffusing state at the end $x = L$.

the particle undergoes normal diffusion (additive noise) so there is no ambiguity in the interpretation of the noise. Nevertheless, if one takes the switching rates to depend on spatial position, then in the fast switching limit one obtains Brownian motion with a space-dependent diffusivity of the Ito form. Advances in single-particle tracking (SPT) and statistical methods suggest that particles within the plasma membrane, for example, can switch between different discrete conformational states with different diffusivities [15–17]. Such switching could be due to interactions between proteins and the actin cytoskeleton [18, 19] or due to protein-lipid interactions [20]. However, until the recent study of Ref. [12], there has been no experimental evidence that the switching rates can be space-dependent.

In this paper, motivated by the experimental study of Ref. [12], we extend our previous work on switching diffusivities to analyze its role in the formation of protein concentration gradients. We begin by describing the standard theory of morphogen gradient formation in section II, and then explore how this is affected by space-independent switching diffusivities in section III. We then turn to the alternative mechanism for gradient formation at the subcellular level, which is based on space-dependent switching diffusivities in the absence of a localized source and protein degradation (section IV).

II. PROTEIN CONCENTRATION GRADIENTS WITHOUT SWITCHING DIFFUSIVITIES

A common model of morphogen gradient formation, as exemplified by the Bcd gradient of *Drosophila*, involves a combination of local protein synthesis, diffusion, and protein degradation [21]. The latter mainly arises via binding to receptors in the cell membrane, internalization and subsequent degradation within a cell. The basic reaction-diffusion equation takes the form

$$\frac{\partial C(x,t)}{\partial t} = D\frac{\partial^2 C(x,t)}{\partial x^2} - kC(x,t) + Q(x), \qquad (2.1)$$

where $C(x,t)$ denotes the concentration of protein, t is the time from the onset of morphogen synthesis, and x, $0 < x < L$, is the distance from the anterior pole of the embryo whose size is L. The total rate of degradation is given by k, and $Q(x)$ represents the spatial distribution of protein synthesis, which is usually approximated by a decaying exponential $Q(x) = (Q_0/\lambda_p)\mathrm{e}^{-x/\lambda_p}$. The initial and boundary conditions are

$$D\frac{\partial C(0,t)}{\partial x} = 0 = D\frac{\partial C(L,t)}{\partial x}, \quad C(0,x) = 0. \qquad (2.2)$$

Experimentally it is observed that the protein concentration decays to zero before reaching the posterior end, so the solution is approximately independent of L. Suppose that morphogen synthesis is strongly localized at the anterior end, $Q(x) = Q_0\delta(x)$, which can be implemented using the modified boundary condition

$$-D\frac{\partial C(0,t)}{\partial x} = Q_0.$$

The steady-state solution then takes the form

$$C^*(x) = C^*(0)\left(\frac{\mathrm{e}^{x/\lambda} + \mathrm{e}^{2L/\lambda}\mathrm{e}^{-x/\lambda}}{\mathrm{e}^{2L/\lambda} - 1}\right), \quad \lambda = \sqrt{\frac{D}{k}}. \qquad (2.3)$$

The constant $C^*(0)$ can be determined from the boundary condition at $x = 0$. In particular, when $L \gg \lambda$, the concentration decays exponentially with length constant λ,

$$C^*(x) = \frac{Q_0\lambda}{D}\mathrm{e}^{-x/\lambda}, \quad \lambda = \sqrt{D/k}. \qquad (2.4)$$

In the case of Bcd, one finds that $D \sim 1\mu m^2/s$, $k^{-1} \sim 1$ hour and $\lambda \sim 75\mu m$. This length constant is too large for subcellular processes [11]. For example, the length of a general eukaryotic cell is typically around 10μm in diameter and the *C. elegans* embryo is typically 30-40 μm.

An important quantity in characterizing the time-dependent approach to steady-state of a diffusion process is the *accumulation time*. In particular, this is used is to estimate the time to form a protein concentration gradient during morphogenesis, which has to be consistent with developmental time scales. In order to construct the accumulation time, consider the function

$$R(x,t) = 1 - \frac{C(x,t)}{C^*(x)}, \qquad (2.5)$$

which represents the fractional deviation of the concentration from the steady-state. Assuming that there is no overshooting, $1 - R(x,t)$ is the fraction of the steady-state concentration that has accumulated at x by time t.

It follows that $-\partial_t R(x,t)dt$ is the fraction accumulated in the interval $[t, t+dt]$. The accumulation time is then defined by analogy to MFPTs [22–24]

$$\tau(x) = \int_0^\infty t\left(-\frac{\partial R(x,t)}{\partial t}\right)dt = \int_0^\infty R(x,t)dt. \quad (2.6)$$

Note that a finite accumulation time implies that the steady-state $C^*(x)$ is a stable solution to (2.1).

As a simple illustration of calculating $\tau(x)$, consider the classical model of morphogen gradient formation

$$\frac{\partial C(x,t)}{\partial t} = D\frac{\partial^2 C(x,t)}{\partial x^2} - kC(x,t), \quad (2.7)$$

where $C(x,t)$ denotes the concentration of a protein, t is the time from the onset of morphogen synthesis, and x, $0<x<L$, is the distance from the anterior pole of an embryo whose size is L. The total rate of degradation is given by k. The initial and boundary conditions are

$$-D\frac{\partial C(0,t)}{\partial x} = Q_0, \quad D\frac{\partial C(L,t)}{\partial x} = 0, \quad C(x,0) = 0. \quad (2.8)$$

The time-dependent solution of Eq. (2.7) for $L\to\infty$ is given by

$$C(x,t) = C^*(x)\left[1 - \frac{1}{2}\mathrm{erfc}\left(\frac{\sqrt{Dt}}{\lambda} - \frac{x}{2\sqrt{Dt}}\right) - \frac{\mathrm{e}^{x/\lambda}}{2}\mathrm{erfc}\left(\frac{\sqrt{Dt}}{\lambda} + \frac{x}{2\sqrt{Dt}}\right)\right],$$

where $\mathrm{erfc}(z)$ is the complementary error function and $\lambda = \sqrt{D/k}$. It follows that

$$R(x,t) = \frac{1}{2}\mathrm{erfc}\left(\frac{\sqrt{Dt}}{\lambda} - \frac{x}{2\sqrt{Dt}}\right) - \frac{\mathrm{e}^{x/\lambda}}{2}\mathrm{erfc}\left(\frac{\sqrt{Dt}}{\lambda} + \frac{x}{2\sqrt{Dt}}\right),$$

and [22]

$$\tau(x) = \frac{1}{2k}(1 + x/\lambda). \quad (2.9)$$

In the case of Bcd, one finds that if $\lambda \sim 75\mu m$ and the most distal region of Bcd expression is at $x = 150\mu m$, then $x_{\max}/\lambda \approx 2$ and $\tau(x_{\max}) \approx 1.5/k$. This would be consistent with the time-scale of gradient formation, which is of the order of an hour.

Summarizing, the standard theory of morphogen gradient formation involving production at a localized source, diffusion, and degradation can indeed account for the Bcd gradient of *Drosophila* and other developmental systems of sufficiently large spatial scales. In the next section, we consider how switching diffusivities modifies this theory.

III. SPACE-INDEPENDENT SWITCHING DIFFUSIVITIES

Now suppose that we have a population of diffusing particles that independently switch between two conformational states labeled $n = 0, 1$ according to a two-state jump Markov process $N(t) \in \{0,1\}$, with $0 \underset{\alpha}{\overset{\beta}{\rightleftharpoons}} 1$. The diffusion coefficient is taken to depend on the conformational state, that is $D = D_n$ when $N(t) = n$ [25–27]. At the population level we have the densities $C_n(x,t)$, $n = 0, 1$, which evolve according to

$$\frac{\partial C_0}{\partial t} = D_0\frac{\partial^2 C_0}{\partial x^2} - (\beta + k)C_0 + \alpha C_1 \quad (3.1a)$$

$$\frac{\partial C_1}{\partial t} = D_1\frac{\partial^2 C_1}{\partial x^2} + \beta C_0 - (\alpha + k)C_1, \quad (3.1b)$$

with

$$-D_0\partial_x C_0(0,t) = Q_0, \quad \partial_x C_1(0,t) = 0, \quad (3.1c)$$

$$\partial_x C_0(L,t) = \partial_x C_1(L,t) = 0. \quad (3.1d)$$

We assume that at $x = 0$ all proteins are produced in the $n = 0$ state at a rate Q_0. Finally, we take the initial condition $C_n(x,0) = 0$ for all x.

Note that the total amount of protein is independent of α, β, D_0, and D_1. To see this, define

$$T(t) = \int_0^L \sum_n C_n(x,t)dx. \quad (3.2)$$

Differentiating with respect to time and using Eqs. (3.1a)–(3.1d) results in

$$\frac{dT}{dt} = \int_0^L \sum_n D_n\frac{\partial^2 C_n}{\partial x^2}dx - k\int_0^L \sum_n C_n dx. \quad (3.3)$$

Enforcing the Neumann boundary conditions for C_0 and C_1 at $x = 0, L$, leads to the equation

$$\frac{dT}{dt} = Q_0 - kT, \quad (3.4)$$

whose solution is $T(t) = Q_0(1 - e^{-kt})/k$. This only depends on the decay rate k, and the influx of protein at the left boundary, given by Q_0.

A. Steady-state gradient and accumulation time

We would like to determine how switching diffusivities affect the accumulation time defined in section II. We will proceed by Laplace transforming Eqs. (3.1a)–(3.1d) with

$$\widehat{C}_n(x,s) = \int_0^\infty \mathrm{e}^{-st}C_n(x,t)dt.$$

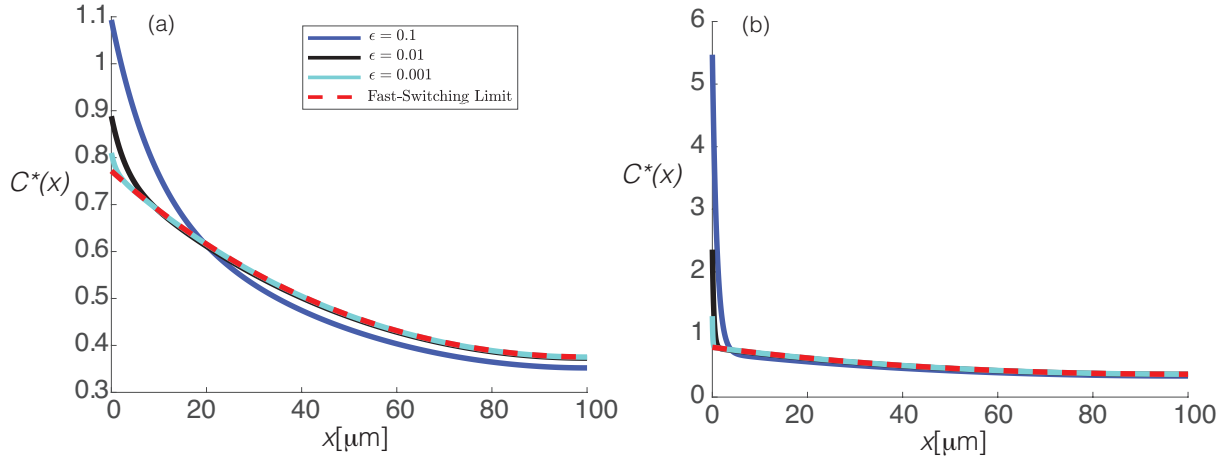

FIG. 2. Comparison of the fast-switching limit to the steady-state solution for various values of ϵ. (a) $\eta = 0.1$ and (b) $\eta = 10^{-3}$. Other parameters are $L = 100\ \mu m$, and $Q_0 = 5 \times 10^{-3}\ [C]\mu m/s$.

This gives

$$s\widehat{C}_0(x,s) = D_0\frac{\partial^2\widehat{C}_0}{\partial x^2} - (\beta+k)\widehat{C}_0(x,s) + \alpha\widehat{C}_1(x,s) \tag{3.5a}$$

$$s\widehat{C}_1(x,s) = D_1\frac{\partial^2\widehat{C}_1}{\partial x^2} + \beta\widehat{C}_0(x,s) - (\alpha+k)\widehat{C}_1(x,s), \tag{3.5b}$$

with $C_n(x,0) = 0$, and

$$-D_0\partial_x\widehat{C}_0(0,s) = s^{-1}Q_0, \quad \partial_x\widehat{C}_1(0,s) = 0, \tag{3.5c}$$

$$\partial_x\widehat{C}_0(L,s) = \partial_x\widehat{C}_1(L,s) = 0. \tag{3.5d}$$

For the sake of illustration, suppose $D_0 = D_1 = D$ and set $C(x,t) = C_0(x,t) + C_1(x,t)$. (The case $D_0 \neq D_1$ is analyzed in the appendix.) Adding Eqs. (3.5a) and (3.5b) gives

$$D\frac{d^2\widehat{C}}{dx^2} - (s+k)\widehat{C} = 0,$$
$$-D\partial_x\widehat{C}(0,s) = s^{-1}Q_0, \quad \partial_x\widehat{C}(L,s) = 0.$$

This recovers the Laplace transformed equations of the non-switching case. It follows that

$$\widehat{C}(x,s) = \frac{Q_0}{sD}\frac{1}{\sqrt{(s+k)/D}} \times \frac{e^{\sqrt{(s+k)/D}(L-x)} + e^{-\sqrt{(s+k)/D}(L-x)}}{e^{\sqrt{(s+k)/D}L} - e^{-\sqrt{(s+k)/D}L}}. \tag{3.6}$$

We immediately obtain the steady-state solution

$$C^*(x) = \lim_{s\to 0} s\widehat{C}(x,s) = \frac{Q_0\lambda}{D}\frac{\cosh([L-x]/\lambda)}{\sinh(L/\lambda)}, \tag{3.7}$$

which agrees with (2.3). Setting

$$\widehat{F}(x,s) = s\widehat{C}(x,s),$$

and Laplace transforming Eq. (2.5) yields

$$s\widehat{R}(x,s) = 1 - \frac{\widehat{F}(x,s)}{\widehat{F}(x,0)},$$

and

$$\tau(x) = \lim_{s\to 0}\widehat{R}(x,s) = \lim_{s\to 0}\frac{1}{s}\left[1 - \frac{\widehat{F}(x,s)}{\widehat{F}(x,0)}\right] = -\frac{1}{\widehat{F}(x,0)}\left.\frac{d}{ds}\widehat{F}(x,s)\right|_{s=0}. \tag{3.8}$$

Using Eq. (3.6) we obtain the result

$$\tau(x) = \frac{1}{2k}\left[1 - \frac{L-x}{\lambda}\tanh([L-x]/\lambda) + \frac{L}{\lambda\tanh(L/\lambda)}\right]. \tag{3.9}$$

Hence, for this particular example the accumulation time is independent of the switching rate. In particular, we recover the result (2.9) in the limit $L \to \infty$.

B. Dependence on switching rate

In order to understand the effects of switching diffusivities on the protein concentration gradient, we need to determine the corresponding system in the fast switching limit $\alpha, \beta \to \infty$ with α/β fixed. The fast-switching limit can be implemented by rescaling the transition rates according to $\alpha, \beta \to \alpha/\epsilon, \beta/\epsilon$, with $\alpha, \beta = O(1)$, and taking $\epsilon \to 0$. This yields the following equation for C:

$$\frac{\partial C}{\partial t} = \overline{D}\frac{\partial^2 C}{\partial x^2} - kC, \tag{3.10}$$

where

$$\overline{D} = \sum_{n=0,1} D_n\rho_n, \quad \rho_0 = 1 - \rho_1 = \frac{\alpha}{\alpha+\beta}. \tag{3.11}$$

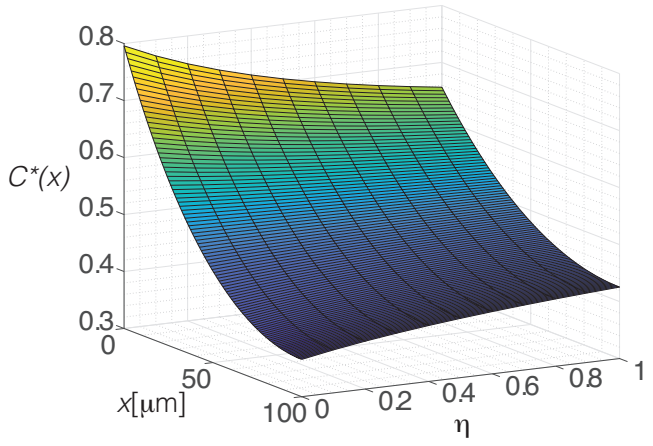

FIG. 3. The fast-switching limit as a function of η. Parameters are $L = 100\ \mu m$ and $Q_0 = 5 \times 10^{-3}\ [C]\mu m/s$.

The corresponding boundary conditions are

$$-\overline{D}\partial_x C(0,t) = Q_0, \quad \partial_x C(L,t) = 0. \tag{3.12}$$

Eq. (3.7) implies that the steady-state solution in the fast switching limit is

$$C^*(x) = \frac{Q_0\overline{\lambda}}{\overline{D}} \frac{\cosh([L-x]/\overline{\lambda})}{\sinh(L/\overline{\lambda})}, \quad \overline{\lambda} = \sqrt{\overline{D}/k}. \tag{3.13}$$

Suppose that we take the baseline parameter values $D = 1\,\mu m^2/s$ and $k = 10^{-4}\,s^{-1}$ with a corresponding length constant $\lambda = \sqrt{D/k} = 100\,\mu m$. For the sake of illustration, we set $\alpha = \beta = k/\epsilon$, $D_1 = D$ and $D_0 = \eta D$ for $0 < \eta < 1$. It follows that $\overline{D} = (1+\eta)D/2$. We explore how the concentration gradient varies with ϵ and η.

Firstly, since the switching rates are taken to be symmetric, in the limit $\eta \to 1$, equations (3.1a) and (3.1b) are identical, meaning that the equilibrium solution is always identical to the fast-switching limit given by (3.7). If we take $\eta = 0.1$, however, the convergence to the fast-switching limit is apparent (Fig. 2(a)). It is important to note that the fast-switching limit gives a more uniform protein concentration gradient than for larger ϵ, which might not be ideal for setting up spatial variation. At $\eta = 0.001$, this difference is even more extreme, but the gradient decays so rapidly that there is only a very narrow region where the protein concentration is high (Fig. 2(b)). Taking the diffusivities to be different orders of magnitude is a way to increase the spatial variation, even in the case of fast-switching. This is illustrated in Fig. 3.

Hence, while the standard theory involving production, diffusion, and degradation can yield morphogen gradients (reviewed in Section II above), we have shown in this section that switching diffusivities can steepen these gradients. In the next section, we show that space-dependent switching diffusivities can yield morphogen gradients in the absence of production and degradation.

IV. SPACE-DEPENDENT SWITCHING DIFFUSIVITIES

So far we have assumed that the morphogen gradient is represented by a protein concentration profile, which is produced by a localized source, diffuses and is uniformly degraded. We now turn to an alternative mechanism, which is based on space-dependent switching diffusivities in the absence of a localized source or degradation. We recently hypothesized that space-dependent switching diffusivities could provide a mechanism for multiplicative noise in the fast switching limit [13, 14], and developed a mathematical analysis of this process. Independently, an experimental and computational modeling study of cell polarization in *C. elegans* showed how such a mechanism could lead to the formation of a morphogen gradient [12]. Here we apply our previous analysis to the latter process. The new system of equations is

$$\frac{\partial C_0}{\partial t} = D_0 \frac{\partial^2 C_0}{\partial x^2} - \beta(x)C_0 + \alpha(x)C_1 \tag{4.1a}$$

$$\frac{\partial C_1}{\partial t} = D_1 \frac{\partial^2 C_1}{\partial x^2} + \beta(x)C_0 - \alpha(x)C_1, \tag{4.1b}$$

with

$$\partial_x C_0(0,t) = \partial_x C_1(0,t) = 0,\ \partial_x C_0(L,t) = \partial_x C_1(L,t) = 0. \tag{4.1c}$$

and the initial conditions $C_n(x,0) = C_n^*$.

A. Fast switching regime

Following our previous work [13, 14], we begin by considering the fast switching limit $\alpha(x), \beta(x) \to \infty$. A typical length of *C. elegans* is around $L = 32\ \mu m$ and the switching rates are of the order $0.1\ s^{-1}$ [12]. Introducing the fundamental time-scale $\tau = L^2/D$ with $D = 1\ \mu m^2/s$, we have $\tau \sim 1000\ s$ and thus the switching rates are at least two orders of magnitude faster than τ^{-1}. Hence, as in section III, we rescale the transition rates according to $\alpha, \beta \to \alpha/\epsilon, \beta/\epsilon$, with $\alpha, \beta = O(1)$. For small but non-zero ϵ, one can use an adiabatic approximation to reduce the diffusion Eqs. (4.1a) and (4.1b) to a corresponding scalar diffusion equation for the total density $C(x,t) = \sum_{n=0,1} C_n(x,t)$ [28, 29]. The basic steps are as follows.

First, decompose the density C_n as

$$C_n(x,t) = C(x,t)\rho_n(x) + \epsilon w_n(x,t), \tag{4.2}$$

where $\sum_n w_n(x,t) = 0$ and

$$\rho_0(x) = \frac{\alpha(x)}{\alpha(x)+\beta(x)}, \quad \rho_1(x) = 1 - \rho_0(x).$$

Substituting this decomposition into Eqs. (4.1a) and (4.1b), and then adding the pair of equations gives

$$\frac{\partial C}{\partial t} = \frac{\partial^2 \overline{D}(x) C}{\partial x^2} + \epsilon \sum_{n=0,1} D_n \frac{\partial^2 w_n}{\partial x^2}, \tag{4.3}$$

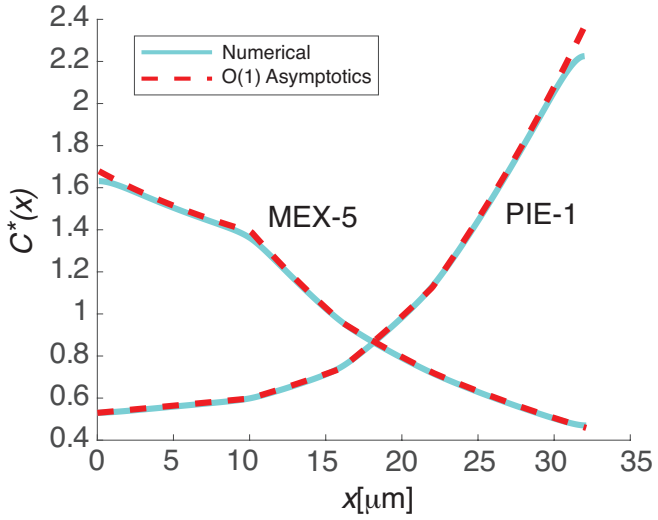

	a_i^M	$\bar{a}_i^M$	a_i^P	$\bar{a}_i^P$
i = 0	0.46	0.004	0.10	0.004
i = 1	0.50	- 0.027	0.14	- 0.01
i = 2	0.20	- 0.017	0.20	- 0.027
i = 3	0.36	- 0.014	0.36	- 0.042

b^M	$\bar{b}^M$	b^P	$\bar{b}^P$
0.10	0.0046	0.2	- 0.0036

FIG. 4. Plot of numerical solution and first order asymptotics for MEX-5 and PIE-1 spatial switching rates given by Eqs. (4.11) and (4.12), respectively, with the values of the coefficients listed in the tables. Parameter values are taken from [12], which were chosen to match their experimental measurements of protein concentrations.

where

$$\overline{D}(x) = \sum_{n=0,1} D_n \rho_n(x). \tag{4.4}$$

Next we use Eq. (4.3) to eliminate $\partial C/\partial t$ in the expanded version of Eqs. (4.1a) and (4.1b). Introducing the asymptotic expansion $w_n \sim w_n^{(0)} + \epsilon w_n^{(1)} + O(\epsilon^2)$ and collecting the $O(1)$ terms then yields an equation for $w_n^{(0)}$, which has the following unique solution on imposing the condition $\sum_n w_n^{(0)}(x,t) = 0$,

$$w_n^{(0)} = \frac{1}{\alpha(x)+\beta(x)}\left[D_n \frac{\partial^2 \rho_n(x) C}{\partial x^2} - \rho_n(x)\frac{\partial^2 \overline{D}(x) C}{\partial x^2}\right]. \tag{4.5}$$

Finally, setting $w_n = w_n^{(0)} + O(\epsilon)$ in Eq. (4.3) shows that to $O(\epsilon)$

$$\frac{\partial C}{\partial t} = \frac{\partial^2}{\partial x^2}(\overline{D}(x)C) + \epsilon(D_0 - D_1)\frac{\partial^2 w_0^{(0)}}{\partial x^2}. \tag{4.6a}$$

However, there is one subtle point that needs to be highlighted. The original system given by Eqs. (4.1a) and (4.1b) involves two coupled diffusion equations so that at each boundary there are two boundary conditions, namely zero flux conditions for C_0 and C_1. On the other hand, the reduced diffusion equation (4.6a) for the scalar $C = C_0 + C_1$ has a single boundary condition at each end. If we take this to be the linear combination $D_0\partial_x C_0 + D_1 \partial_x C_1 = 0$ and substitute the decomposition (4.2), then we obtain the non-flux conditions

$$\partial_x[\overline{D}(x)C(x,t) + \epsilon(D_0 - D_1)w_0^{(0)}]_{x=0} = 0 \tag{4.6b}$$

$$\partial_x[\overline{D}(x)C(x,t) + \epsilon(D_0 - D_1)w_0^{(0)}]_{x=L} = 0. \tag{4.6c}$$

We thus have a singular perturbation problem, in which the solution to Eqs. (4.6) represents an outer solution that is valid in the bulk of the domain, but has to be matched to an inner solution at each boundary. (An analogous situation holds in mathematical models of bidirectional motor transport [29, 30].) We will address this issue further below, but first we focus on the bulk solution in the limit $\epsilon \to 0$.

In the fast switching limit $\epsilon \to 0$, we have a diffusion equation with effective space-dependent diffusivity $\overline{D}(x)$:

$$\frac{\partial C}{\partial t} = \frac{\partial^2}{\partial x^2}(\overline{D}(x)C), \tag{4.7}$$

with no-flux boundary conditions $\partial_x \overline{D}(x)C(x,t) = 0$ at $x = 0, L$. It is now straightforward to establish that the bulk solution can take the form of a protein concentration gradient. The steady-state solution takes the form

$$C^*(x) = \frac{A}{\overline{D}(x)}, \tag{4.8}$$

with the constant A determined by the normalization condition

$$\int_0^L C^*(x)dx = L[C_0^* + C_1^*]. \tag{4.9}$$

Hence,

$$A = L[C_0^* + C_1^*]\left[\int_0^L \frac{dx}{\overline{D}(x)}\right]^{-1}. \tag{4.10}$$

It is clear that regions of slow diffusion will have higher concentrations than regions of fast diffusion. Suppose for the sake of illustration that $D_0 < D_1$. This means that

$\overline{D}(x)$ will be a monotonically increasing function of x if $\alpha(x)$ is a constant or a decreasing function of x and $\beta(x)$ is an increasing function of x; the resulting stationary concentration will be a monotonically decreasing function of x. This will be illustrated in section IV.C.

B. Examples of switching rates

Substituting the switching rates found in [12] for the RNA-binding proteins MEX-5 and PIE-1 gives the following numerical and first order asymptotics results. The switching rates are both between 0.1 s^{-1} and 0.8 s^{-1} at each point in the domain. The other parameters are given by $D_0 = 0.1\ \mu m^2/s$, $D_1 = 5\ \mu m^2/s$, and $L = 32\ \mu m$, as in [12]. In both cases, we approximate the switching rates using piecewise constant functions. That is, the interval is divided into four subintervals $I_i = [x_i, x_{i+1}), i = 0, \ldots, 3$ with $x_0 = 0$ $x_1 = 10$, $x_2 = 16$, $x_3 = 22$ and $x_4 = L$ such that

$$\begin{aligned} &\alpha_M(x) = a_i^M + \bar{a}_i^M(x - x_i) \text{ for } x \in I_i, \quad i = 0, \ldots, 3 \\ &\beta_M(x) = b^M + \bar{b}^M x, \quad x \in [0, L] \end{aligned} \tag{4.11}$$

for MEX-5 and

$$\begin{aligned} &\alpha_P(x) = a_i^P + \bar{a}_i^P(x - x_i) \text{ for } x \in I_i, \quad i = 0, \ldots, 3 \\ &\beta_P(x) = b^P, \quad x \in [0, x_1] \\ &\beta_P(x) = b^P + \bar{b}^P(x - x_1), \quad x \in [x_1, L] \end{aligned} \tag{4.12}$$

for PIE-1. The various coefficients are listed in the tables of Fig. 4. Note that the first order asymptotics well-approximate the steady-state concentration since there is already a fast time scale based on the biological parameters as outlined at the beginning of this section. This is illustrated in Fig. 4. We emphasize that our numerical results in Fig. 4 are consistent with the numerical results of Wu et al. [12], which closely matched their experimental measurements of protein concentrations. Furthermore, all the parameter values are taken from [12], which were chosen to match their experimental results.

C. Boundary layer analysis

In order to solve the steady-state singular perturbation problem, we introduce an $O(\sqrt{\epsilon})$ boundary layer at $x = 0$ and similarly at $x = L$, which can capture rapid changes in spatial derivatives. We then construct an inner solution within each boundary layer that can then be matched to the outer solution of Eqs. (4.6). For the sake of illustration, we focus on the boundary layer at $x = 0$; the analysis for the other boundary layer is very similar. Introduce the stretched coordinate

$$X = \frac{x}{\sqrt{\epsilon}}. \tag{4.13}$$

and series expansions

$$\alpha(\sqrt{\epsilon}X) \sim \alpha_0 + \alpha_1\sqrt{\epsilon}X + O(\epsilon) \tag{4.14a}$$
$$\beta(\sqrt{\epsilon}X) \sim \beta_0 + \beta_1\sqrt{\epsilon}X + O(\epsilon) \tag{4.14b}$$

Denote the steady-state inner solution by $C_{\text{in}}^*(X)$, which is taken to have the series expansion

$$C_{\text{in}}^*(X) \sim c_{n,0}(X) + \sqrt{\epsilon}c_{n,1}(X) + O(\epsilon). \tag{4.14c}$$

The steady-state version of Eqs. (4.6) yields, to leading order, the following inner equations on the domain $X \in [0, \infty)$:

$$0 = D_0\frac{d^2c_{0,0}}{dX^2} - \beta_0 c_{0,0} + \alpha_0 c_{1,0} \tag{4.15a}$$
$$0 = D_1\frac{d^2c_{1,0}}{dX^2} + \beta_0 c_{0,0} - \alpha_0 c_{1,0}, \tag{4.15b}$$

with boundary conditions $c'_{0,0}(0) = c'_{1,0}(0) = 0$. Adding Eqs. (4.15a) and (4.15b) and imposing the boundary conditions shows that $\sum_{n=0,1} D_n c_{n,0}(X) = \Gamma_0$, where Γ_0 is a constant. Eq. (4.15a) can thus be rewritten as

$$0 = \frac{d^2c_{0,0}}{dX^2} - \left(\frac{\beta_0}{D_0} + \frac{\alpha_0}{D_1}\right)c_{0,0} + \frac{\alpha_0\Gamma_0}{D_0D_1}. \tag{4.16}$$

This has the bounded solution

$$c_{0,0}(X) = A_0 e^{-\gamma X} + \frac{\alpha_0\Gamma_0}{D_0D_1\gamma}, \tag{4.17}$$

with

$$\gamma = \sqrt{\frac{\beta_0}{D_0} + \frac{\alpha_0}{D_1}} = \sqrt{\frac{\overline{D}(0)}{D_0D_1}(\alpha_0 + \beta_0)}. \tag{4.18}$$

The boundary condition $c'_{0,0}(0)$ implies that $A_0 = 0$. Carrying out a similar analysis for $c_{1,0}$ we deduce that the lowest order terms are constants, that is, $c_{n,0}(X) = \overline{c}_n$ with:

$$\overline{c}_n = \frac{\rho_n(0)\Gamma_0}{\overline{D}(0)}.$$

Proceeding to the next order, we have

$$\beta_1 X\overline{c}_0 - \alpha_1 X\overline{c}_1 = D_0\frac{d^2c_{0,1}}{dX^2} - \beta_0 c_{0,1} + \alpha_0 c_{1,1} \tag{4.19a}$$

$$-\beta_1 X\overline{c}_0 + \alpha_1 X\overline{c}_1 = D_1\frac{d^2c_{1,1}}{dX^2} + \beta_0 c_{0,1} - \alpha_0 c_{1,1}, \tag{4.19b}$$

with boundary conditions $c'_{0,1}(0) = c'_{1,1}(0) = 0$. Again adding equations (4.19a) and (4.19b) shows that $\sum_{n=0,1} D_n c_{n,1}(X) = \Gamma_1$ for some constant Γ_1. Hence, Eq. (4.19a) becomes

$$\begin{aligned} &\frac{d^2c_{0,1}}{dX^2} - \left(\frac{\beta_0}{D_0} + \frac{\alpha_0}{D_1}\right)c_{0,1} + \frac{\alpha_0\Gamma_1}{D_0D_1} \\ &\qquad = (\beta_1\rho_0(0) - \alpha_1\rho_1(0))\frac{\Gamma_0 X}{D_0\overline{D}(0)}. \end{aligned} \tag{4.20}$$

The bounded solutions are

$$c_{0,1}(X) = B_0 \mathrm{e}^{-\gamma X} - \frac{D_1\left(\beta_1\alpha_0 - \alpha_1\beta_0\right)}{(\alpha_0+\beta_0)^2}\frac{\Gamma_0 X}{\overline{D}(0)^2} \tag{4.21}$$

and, similarly,

$$c_{1,1}(X) = B_1 \mathrm{e}^{-\gamma X} + \frac{D_0\left(\beta_1\alpha_0 - \alpha_1\beta_0\right)}{(\alpha_0+\beta_0)^2}\frac{\Gamma_0 X}{\overline{D}(0)^2}. \tag{4.22}$$

Without loss of generality we have set $\Gamma_1 = 0$. The coefficients B_0 and B_1 can be determined in terms of Γ_0 by imposing the non-flux boundary conditions at $X = 0$.

Combining our various results and using the definition of $\overline{D}(x)$ leads to the following inner solution

$$\begin{aligned} C^*_{\text{in}}(X) &\sim B\mathrm{e}^{-\gamma X} + \Gamma_0\left(\frac{1}{\overline{D}(0)} - \sqrt{\epsilon}\frac{X\overline{D}'(0)}{\overline{D}(0)^2}\right) + O(\epsilon) \\ &\sim B\mathrm{e}^{-\gamma X} + \frac{\Gamma_0}{\overline{D}(\sqrt{\epsilon}X)}. \end{aligned} \tag{4.23}$$

The boundary condition $dC^*_{\text{in}}(X)/dX = 0$ at $X = 0$ shows that

$$B = -\frac{\Gamma_0\overline{D}'(0)}{\gamma\overline{D}(0)^2}. \tag{4.24}$$

The composite solution then has the form

$$C^*(x) = \frac{A}{\overline{D}(x)} + \sqrt{\epsilon}B\mathrm{e}^{-\gamma x/\sqrt{\epsilon}}, \tag{4.25}$$

with the matching condition $\Gamma_0 = A$.

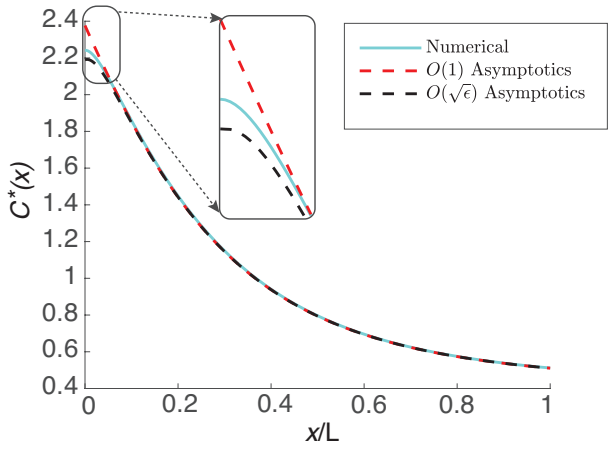

FIG. 5. Equilibrium density with switching rates given by $\alpha(x) = 2$, $\beta(x) = (x + 0.65)^4$. The diffusion coefficients were set to $D_0 = 0.5$, $D_1 = 5$, with $\epsilon = 5 \times 10^{-4}$. The red and black dashed lines show the increased accuracy achieved by the $O(\sqrt{\epsilon})$ terms.

Performing the same boundary analysis for the boundary layer at $x = L$, we find that the composite solution for the entire domain has the form

$$\begin{aligned} C^*(x) = \frac{A}{\overline{D}(x)} &- \sqrt{\epsilon}\frac{A\overline{D}'(0)}{\gamma\overline{D}(0)^2}\mathrm{e}^{-\gamma x/\sqrt{\epsilon}} \\ &+\sqrt{\epsilon}\frac{A\overline{D}'(L)}{\mu\overline{D}(L)^2}\mathrm{e}^{-\mu(L-x)/\sqrt{\epsilon}}, \end{aligned} \tag{4.26}$$

where we have defined

$$\mu = \sqrt{\frac{\beta(L)}{D_0} + \frac{\alpha(L)}{D_1}} = \sqrt{\frac{\overline{D}(L)}{D_0 D_1}\left(\alpha(L) + \beta(L)\right)}. \tag{4.27}$$

Note that the correction to the normalization constant A given in (4.10) is of $O(\epsilon)$, and hence does not need to be included here at $O(\sqrt{\epsilon})$. For small ϵ, these terms result in an increased accuracy near the boundary by helping enforce the no-flux boundary conditions in the asymptotic solution. Fig. 5 highlights an example of this improvement.

D. Accumulation time for fast spatial switching

It is also possible to use the bulk equilibrium solution found from Eq. (4.7) in the limit of fast switching to calculate an approximation for the accumulation time $\tau(x)$. This can be done even with the presence of spatially dependent switching rates with a slight modification to the function $R(x,t)$. Since the total protein amount is conserved when no-flux boundary conditions are present, and the initial protein concentration gradient

$$C^*_{\text{init}} := C^*_0 + C^*_1 \tag{4.28}$$

is non-zero, it is inevitable that $C^*_{\text{init}} > C^*(x)$ in some region of the spatial domain. We therefore define

$$R(x,t) = \frac{C^*(x) - C(x,t)}{C^*(x) - C^*_{\text{init}}} = 1 - \frac{C(x,t) - C^*_{\text{init}}}{C^*(x) - C^*_{\text{init}}}. \tag{4.29}$$

Again assuming there is no overshooting, this is the fractional deviation of the concentration from the steady-state. However, it is important to note that there is a slight overshooting in the total concentrations of both MEX-5 and PIE-1 near where $C^*_{\text{init}} = C^*(x)$. Since $\overline{D}(x)$ is monotonic for both PIE-1 and MEX-5, there is only a single value of x where this occurs, which is at approximately $x = 16\ \mu m$ for MEX-5 and $x = 20\ \mu m$ for PIE-1. Figs. (6). However, this issue is not present farther away from these spatial points, so we will focus on deriving the accumulation time for values of x away from where $C^*(x) = C^*_{\text{init}}$.

The accumulation time can be calculated by utilizing the Laplace transform like before, with the final equation being given by

$$\tau(x) = \frac{-1}{C^*(x) - C^*_{\text{init}}}\left.\frac{d}{ds}\widehat{F}(x,s)\right|_{s=0}, \tag{4.30}$$

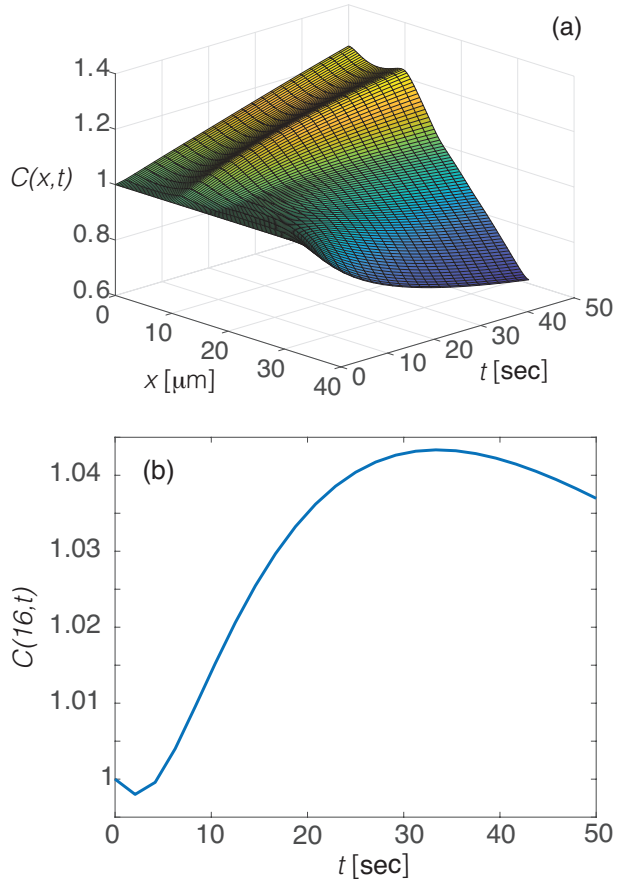

FIG. 6. (a) MEX-5 concentration over space and time. (b) MEX-5 concentration plotted versus time t at $x = 16$ μm showing slight overshooting. Initial state concentrations are $C_0^* = 0.75$, $C_1^* = 0.25$.

where $\widehat{F}(x,s) = s\widehat{C}(x,s)$ and thus $\widehat{F}(x,0) = C^*(x)$. Although there is no general formula for the time-dependent solution to Eq. (4.7), we can use the latter to derive a differential equation for

$$\widehat{F}_s^0(x) := \frac{d}{ds}\widehat{F}(x,s)\bigg|_{s=0}. \tag{4.31}$$

First, Laplace transforming (4.7) and multiplying both sides by s results in

$$\frac{\partial^2 \overline{D}(x)\widehat{F}}{\partial x^2} = s\widehat{F} - sC^*_{\text{init}}. \tag{4.32}$$

Assuming derivatives commute, we can take the derivative with respect to s, yielding

$$\frac{\partial^2 \overline{D}(x)\widehat{F}_s}{\partial x^2} = \widehat{F} + s\widehat{F}_s - C^*_{\text{init}}. \tag{4.33}$$

In the limit $s \to 0^+$, we have that $\widehat{F}_s$ exists and is finite, therefore

$$\lim_{s\to 0^+} s\widehat{F}_s = 0. \tag{4.34}$$

We now have an equation

$$\frac{\partial^2 \overline{D}(x)\widehat{F}_s^0}{\partial x^2} = C^*(x) - C^*_{\text{init}} \tag{4.35a}$$

that describes $\widehat{F}_s^0$ in terms of the equilibrium protein concentration gradient and the initial distribution of protein. Using a similar approach combined with the fact that total protein is conserved, we derive boundary conditions

$$\partial_x[\overline{D}(x)\widehat{F}_s^0(x)]_{x=0} = 0 \tag{4.35b}$$
$$\partial_x[\overline{D}(x)\widehat{F}_s^0(x)]_{x=L} = 0, \tag{4.35c}$$

and a homogenization condition

$$\int_0^L \widehat{F}_s^0(x)dx = 0. \tag{4.35d}$$

With Eqs. (4.35a)–(4.35c), we find

$$\widehat{F}_s^0(x) = \frac{1}{\overline{D}(x)}\int_0^x \int_0^{x'} (C^*(x'') - C^*_{\text{init}})\, dx''dx' - \frac{F^*}{\overline{D}(x)} \tag{4.36}$$

with the constant F^* determined by Eq. (4.35d),

$$F^* = \frac{A}{LC^*_{\text{init}}}\int_0^L \overline{D}(x)^{-1} \times \left[\int^x \int^{x'} (C^*(x'') - C^*_{\text{init}})\, dx''dx'\right] dx, \tag{4.37}$$

and A is defined in Eq. (4.10). Finally, from Eq. (4.30), the accumulation time is given by

$$\tau(x) = \frac{F^*}{A - C^*_{\text{init}}\overline{D}(x)} - \frac{1}{A - C^*_{\text{init}}\overline{D}(x)}\int^x \int^{x'} (C^*(x'') - C^*_{\text{init}})\, dx''dx'. \tag{4.38}$$

The same formula holds true if the initial concentration C^*_{init} is taken to be spatially varying rather than constant across the domain. Note that in either case, the accumulation time is singular where $A = C^*_{\text{init}}\overline{D}(x)$, or equivalently where $C^*(x) = C^*_{\text{init}}$. If $C(x^*,t) = C^*_{\text{init}}$ for all time t at some location $x = x^*$, then the accumulation time $\tau(x^*)$ will be zero, however, if there is some slight variation in the concentration over time at $x = x^*$, then $\tau(x)$ will be undefined.

Using numerical integration to calculate (4.38), we find that for MEX-5

$$\tau_M(2) = 72\ s, \quad \tau_M(10) = 39\ s$$
$$\tau_M(25) = 58\ s, \quad \tau_M(30) = 42\ s,$$

and for PIE-1

$$\tau_P(2) = 57\ s, \quad \tau_P(10) = 53\ s$$
$$\tau_P(25) = 55\ s, \quad \tau_P(30) = 57\ s.$$

In both cases, we see that the bulk forms on a timescale of about a minute, regardless of the spatial location. This is consistent with intracellular concentration gradients, which tend to form on a timescale of a few minutes. Therefore, our results indicate that space-dependent switching diffusivities can indeed yield morphogen gradients at both the temporal and the spatial scales relevant to subcellular processes.

V. DISCUSSION

In this paper we studied the role of switching diffusivities in the formation of protein concentration gradients. We assumed that each protein switches between two conformational states with distinct spatially constant diffusivities, and took the switching rates to be space-dependent and faster than the rate of gradient formation. In the fast switching limit this generated an effective space-dependent diffusivity of the Ito form. We then derived explicit expressions for the steady-state intracellular concentration gradient and the associated accumulation time, and showed how these expressions agree with recent experimental and computational results concerning embryogenesis in *C. elegans*.

Although we focused on one specific application in developmental biology, the underlying mechanism raises a number of more general issues concerning heterogeneous diffusion in cells and its role in gradient formation. First, it is important to note that the generation of a protein concentration gradient in the absence of a localized source does not require space-dependent switching diffusivities; the essential ingredient is an effective space-dependent diffusivity as expressed by Eq. (4.7). Space-dependent switching is one mechanism for generating such a diffusivity, at least in the fast switching limit. An alternative to this kinetic mechanism is a static mechanism whereby a protein exists in a single diffusive state at a given spatial position, but the diffusion coefficient spatially varies due to heterogeneities in the surrounding cellular medium [31–34]. Advances in single particle tracking experiments and data analysis techniques such as hidden Markov models [17] now provide a framework for distinguishing between kinetic and static cases. Irrespective of the specific source of heterogeneity, there are two additional properties of the diffusive transport that have to be considered: (i) the appropriate interpretation of the nonlinear Brownian motion (multiplicative noise), and (ii) the underlying biophysical mechanism for generating a spatial gradient in the diffusivity.

The interpretation of a stochastic differential equation with a space-dependent diffusion term is a long-standing and recently revisited [35–37] issue in stochastic calculus. The most common interpretations are Itô, Stratonovich, and kinetic (also called isothermal or Hänggi-Klimontovich), and each arises in different physical scenarios. For example, taking the white noise limit of a particle driven by colored noise yields Stratonovich [38], whereas consistency with equilibrium statistical physics yields the kinetic interpretation. Further, the kinetic interpretation is the natural framework of Fick's law, and recent experiments indicate its relevance for particles diffusing near a wall [39–41]. In this paper and previous work [13], we have shown that when a diffusing particle switches between two or more spatially constant diffusivities with fast, space-dependent switching rates, this leads to an effective space-dependent diffusivity of the Ito form, see Eq. (4.7). However, it is also possible to generate other forms of multiplicative noise by considering a colored noise process with switching diffusivities, and taking the white noise and fast switching limits with different scalings [14]. The nature of the multiplicative noise is critical to analyzing protein concentration gradient formation. For example, if the multiplicative noise were of the kinetic form, the concentration $C(x,t)$ would satisfy a diffusion equation of the form,

$$\frac{\partial C}{\partial t} = \frac{\partial}{\partial x}\Big(\overline{D}(x)\frac{\partial}{\partial x}C\Big). \tag{5.1}$$

The distinction between Eqs. (4.7) and (5.1) is crucial because steady state solutions to (4.7) are proportional to $(\overline{D}(x))^{-1}$, whereas steady state solutions to (5.1) are constant in space. That is, there would be no concentration gradient if the multiplicative noise were kinetic.

Even if the spatially heterogeneous diffusion process evolves according to the Ito interpretation, a protein concentration gradient will only form if there is a corresponding gradient in the rate of diffusion. Therefore, the more general applicability of the mechanism analyzed in this paper will depend on identifying biophysical processes that support a monotonic spatial variation in the effective diffusivity. Here we briefly describe the particular processes thought to hold in the case of *C. elegans* embryogeneisis [12]. Current evidence suggests MEX-5 diffusivity is controlled by differences in the distribution of kinases and phosphotases along the anterior/posterior axis of the zygote. That is, so-called PAR protein kinases in the posterior membrane locally phosphorylate MEX-5, which is then dephosphorylated throughout the cytoplasm by the phosphotase PP2A. The spatial segregation of opposing kinases and phosphatases thus generates a gradient in the phosphorylation state of MEX-5 [42], which is thought to produce local differences in the kinetics of binding/dissociation of MEX-5 from a slow-diffusing substrate, resulting in a corresponding gradient in the effective rate of diffusion. A second phosphorylation cycle operating from the anterior end is likely to be the source of differential diffusion in the case of Pie-1. Since intracellular gradients in the phosphorylation state of a protein are known to play a role in a wide range of cellular processes, including cell division, polarity and mitotic spindle dynamics [10, 11], one might expect there to be other examples where such gradients target the diffusion state of a downstream protein.

APPENDIX A: STEADY-STATE GRADIENT AND ACCUMULATION TIME ($D_0 \neq D_1$)

Here we extend the calculation of Sect. IIIA to the case $D_0 \neq D_1$. It is convenient to rewrite Eqs. (3.5a) and (3.5b) as a second order system

$$\frac{\partial^2}{\partial x^2}\begin{pmatrix}\widehat{C}_0\\ \widehat{C}_1\end{pmatrix} = \begin{pmatrix}(\beta+k+s)/D_0 & -\alpha/D_0\\ -\beta/D_1 & (\alpha+k+s)/D_1\end{pmatrix}\begin{pmatrix}\widehat{C}_0\\ \widehat{C}_1\end{pmatrix}. \tag{A.1}$$

Define the eigenvalues and eigenvectors of the coefficient matrix by $\mu_\pm^2(s)$ and $\vec{v}_\pm(s)$ respectively, where

$$\mu_\pm^2(s) = \frac{\gamma_1(s)+\gamma_2(s)}{2} \pm \frac{1}{2}\sqrt{[\gamma_1(s)-\gamma_2(s)]^2 - 4\eta} \tag{A.2}$$

$$\vec{v}_\pm(s) = \begin{pmatrix}1\\ v_\pm(s)\end{pmatrix}, \tag{A.3}$$

where for convenience γ, μ, and $v_\pm$ are defined as

$$\gamma_1(s) = \frac{\alpha+k+s}{D_1}, \quad \gamma_2(s) = \frac{\beta+k+s}{D_0}, \quad \eta = \frac{\alpha\beta}{D_0 D_1}$$
$$v_\pm(s) = \frac{D_0}{\alpha}\left(\gamma_2(s) - \mu_\pm^2(s)\right).$$

We have written the eigenvalues as squares since the solution of the second-order system will depend on $\mu_\pm$.

The general solution to the above system with boundary conditions (3.5c)–(3.5d) is then

$$\begin{pmatrix}\widehat{C}_0(x,s)\\ \widehat{C}_1(x,s)\end{pmatrix} = \frac{\alpha Q_0}{sD_0^2(\mu_+^2(s)-\mu_-^2(s))}\left[\frac{v_-(s)}{\mu_+(s)}\frac{\cosh(\mu_+(s)[L-x])}{\sinh(\mu_+(s)L)}\vec{v}_+(s) - \frac{v_+(s)}{\mu_-(s)}\frac{\cosh(\mu_-(s)[L-x])}{\sinh(\mu_-(s)L)}\vec{v}_-(s)\right]. \tag{A.4}$$

Note that $\mu_\pm$ is always a positive real number for $\alpha, \beta, D_0, D_1, k > 0$. We can now calculate the steady-state concentration

$$\begin{aligned} C^*(x) &= \lim_{s\to 0} s(\widehat{C}_0(x,s) + \widehat{C}_1(x,s)) \\ &= \frac{\alpha Q_0}{D_0^2(\mu_+^2(0)-\mu_-^2(0))}\left[\frac{(1+v_+(0))v_-(0)}{\mu_+(0)}\frac{\cosh(\mu_+(0)[L-x])}{\sinh(\mu_+(0)L)} - \frac{(1+v_-(0))v_+(0)}{\mu_-(0)}\frac{\cosh(\mu_-(0)[L-x])}{\sinh(\mu_-(0)L)}\right], \end{aligned} \tag{A.5}$$

and the accumulation time $\tau(x)$ using Eq. (3.8). Note that if $D_0 = D_1 = D$ then $\mu_+(0) = \sqrt{(\alpha+\beta+k)/D}$, $\mu_-(0) = \sqrt{k/D} = \lambda^{-1}$, $v_+(s) = -1$, $v_-(s) = \beta/\alpha$ and we recover Eq. (3.7).

ACKNOWLEDGEMENTS

PCB was supported by the National Science Foundation (DMS 1613048) and SDL by the National Science Foundation (DMS 1814832 and DMS-RTG 1148230).

[1] L. Wolpert. Positional information and the spatial pattern of cellular differentiation. J. Theor. Biol. **25** 1–47 (1969).

[2] L. Wolpert, Principles of Development. Oxford, UK: Oxford Univ. Press (2006).

[3] S. Y. Shvartsman and R. E. Baker. Mathematical models of morphogen gradients and their effects on gene expression. Rev. Dev Biol **1** 715–730 (2012).

[4] H. Teimouri and A. B. Kolomeisky. Mechanisms of the formation of biological signaling profiles. J. Phys. A: Math. Theor. **49** 483001 (2016).

[5] A. M. Turing, The chemical basis of morphogenesis, Phil. Trans. Ro. Soc. Series B, Biological Sciences **237** 37-72 (1952).

[6] A. Gierer and H. Meinhardt, A theory of biological pattern formation, Kybernetik, **12** 30–39 (1972).

[7] J. D. Murray, Mathematical biology, Vols. I and II (3rd ed.). Berlin: Springer (2008).

[8] A. N. Zaikin and A. M. Zhabotinsky Concentration wave propagation in two-dimensional liquid-phase self-oscillating system. Nature **225**, 535-537 (1970).

[9] S. Kondo and R. Asai, A reaction-diffusion wave on the skin of the marine angelfish Pomacanthus. Nature **376**, 765-768 (2002).

[10] B. N. Kholodenko. Spatially distributed cell signalling. FEBS Letters **583**, 4006-4012 (2009).

[11] M. Howard. How to build a robust intracellular concentration gradient. Trends Cell Biol **22** 311–317 (2012).

[12] Y. Wu, B. Han, Y. Li, E. Munro, D. J. Odde, and E. E. Griffin. Rapid diffusion-state switching underlies stable cytoplasmic gradients in the Caenorhabditis elegans zygote Proc. Natl. Acad. Sci. USA **115** 8440–8449 (2018).

[13] P. C. Bressloff and S. D. Lawley. Temporal disorder as a mechanism for spatially heterogeneous diffusion. Phys. Rev. E **95** 060101(R) (2017).

[14] P. C. Bressloff and S. D. Lawley. Hybrid colored noise process with space-dependent switching rates. Phys. Rev. E **96** 012129 (2017).

[15] R. Das, C. W. Cairo and D. Coombs, A hidden Markov model for single particle tracks quantifies dynamic interactions between LFA-1 and the actin cytoskeleton. PLoS Comp. Biol. **5** e1000556 (2009)

[16] F. Persson, M. Linden, C. Unoson and J. Elf. Extracting intracellular diffusive states and transition rates from single-molecule tracking data. Nat. Meth. **10** 265 (2013).

[17] P. J. Slater, C. W. Cairo and N. J. Burroughs. Detection of diffusion heterogeneity in single particle tracking trajectories using a hidden Markov model with measurement noise propagation. PLoS ONE **10** e0140759 (2015).

[18] A. Kusumi, C. Nakada, K. Ritchie, K. Murase, K. Suzuki, H. Murakoshi et al. Paradigm shift of the plasma membrane concept from the two-dimensional continuum fluid to the partitioned fluid: high-speed single-molecule tracking of membrane molecules. Ann. Rev. Biophys. Biomol. Struct. **34** 351-378 (2005).

[19] A. Kusumi, K. G. N. Suzuki , R. S. Kasai, K. Ritchieand T. K. Fujiwara, Hierarchical mesoscale domain organization of the plasma membrane. Trends in Biochem. Sci. **36** 604-615 (2011).

[20] E. Yamamoto, T. Akimotot, A. C. Kalli, K. Yasuoka and M. S. P. Sansom. Dynamic interactions between a membrane binding protein and lipids induce fluctuating diffusivity. Sci. Adv. **3** e1601871 (2017).

[21] A. Porcher and N. Dostani. The bicoid morphogen system. Current Biology **20** R249–R254 (2010).

[22] A. M. Berezhkovskii, C. Sample and S. Y. Shvartsman. How long does it take to establish a morphogen gradient? Biophys. J. **99** L59-L61 (2010).

[23] A. M. Berezhkovskii, C. Sample and S. Y. Shvartsman. Formation of morphogen gradients: local accumulation time. Phys Rev E **83** 051906 (2011).

[24] P. Gordon, C. Sample, A. M. Berezhkovskii, C. B. Muratov and S. Y. Shvartsman. Local kinetics of morphogen gradients. Proc Natl Acad Sci **108** 6157-6162 (2011).

[25] The case of space-independent switching between two diffusive states has also been analyzed in Refs. [26, 27]. We could also take the degradation rates to depend on n.

[26] P. C. Bressloff and S. D. Lawley. Residence times of a Brownian particle with temporal heterogeneity. J. Phys. A **50** 195001 (2017).

[27] A. Godec and R. Metzler. First passage time statistics for two-channel diffusion. J. Phys. A **50** 084001 (2017).

[28] G. C. Papanicolaou. Asymptotic analysis of transport processes. Bull. Amer. Math. Soc. **81** 330-392 (1975).

[29] J. M. Newby and P. C. Bressloff. Quasi-steady state reduction of molecular-based models of directed intermittent search. Bull Math Biol **72** 1840-1866 (2010).

[30] C. Zmurchok, T. Small, M. J. Ward and L. Edelstein-Keshet. Application of quasi-steady state methods to nonlinear models of intracellular transport by molecular motors. Bull. Math. Bio, **79** 1923-1978 (2017).

[31] H. A. Soula, A. Coulon and G. Beslon Membrane microdomains emergence through non-homogeneous diffusion, BMC Biohysics **5**, 6 (2012).

[32] H. Berry, C. Manzo and J. A. Torreno-Pina, Spatial distributions at equilibrium under heterogeneous transient subdiffusion, Front. Physiol. **5**, 437 (2014).

[33] P. Massignan, C. Manzo and J. A. Torreno-Pina, Nonergodic subdiffusion from Brownian motion in an inhomogeneous medium, Phys. Rev. Lett. **112** 150603 (2014).

[34] C. Manzo, J. A. Torreno-Pina and P. Massignan, Weak ergodicity breaking of receptor motion in living cells stemming from random diffusivity, Phys. Rev. X **5** 011021 (2015).

[35] R. Mannella and P. V. E. McClintock. Ito vs. Stratonovich - 30 years later. Fluct. Noise Lett. **11**, 1240010 (2012).

[36] P. F. Tupper and X. Yang. A paradox of state-dependent diffusion and how to resolve it. Proc. R. Soc. A 468, 3864 (2012).

[37] G. Vaccario, C. Antione and J.Talbot. First-passage times in d-dimensional heterogeneous media. Phys. Rev. Lett. **115** 240601 (2015).

[38] C. Gardiner, *Handbook of Stochastic Methods*, 3rd. ed. (Springer, New York, 2004).

[39] G. Volpe, L. Helden, T. Brettschneider, J. Wehr, and C. Bechinger. Influence of noise on force measurements. Phys. Rev. Lett. **104**, 170602 (2010).

[40] P. Lancon, G. Batrouni, L. Lobry, and N. Ostrowsky. Drift without flux: Brownian walker with a space dependent diffusion coefficient Europhys. Lett. **54**, 28 (2001).

[41] T. Brettschneider, G. Volpe, L. Helden, J. Wehr, and C. Bechinger. Force measurement in the presence of Brownian noise: Equilibrium-distribution method versus drift method. Phys. Rev. E **83**, 041113 (2011).

[42] E. E. Griffin, D. J. Odde and G. Seydoux. Regulation of the MEX-5 gradient by a spatially segregated kinase/phosphatase cycle. Cell **146** 955-968 (2011).